Krauskopf, B., & Sieber, J. (2003). Bifurcation analysis of an inverted pendulum with delayed feedback control near a triple-zero eigenvalue singularity. DOI: 10.1088/0951-7715/17/1/006

Bifurcation analysis of an inverted pendulum with delayed feedback control near a triple-zero eigenvalue singularity

June 2003

Bernd Krauskopf and Jan Sieber

Bristol Centre for Applied Nonlinear Mathematics, Department of Engineering Mathematics, Queen's Building, University of Bristol, BS8 1TR, U.K.

E-mail: (of corresponding author) Jan.Sieber@bristol.ac.uk

Abstract. We investigate a delay differential equation that models a pendulum stabilized in the upright position by a delayed linear horizontal control force. Linear stability analysis reveals that the region of stability of the origin (the upright position of the pendulum) is bounded for positive delay. We find that a codimension-three triple-zero eigenvalue bifurcation acts as an organizing center of the dynamics. It is studied by computing and then analysing a reduced three-dimensional vector field on the center manifold. The validity of this analysis is checked in the full delay model with the continuation software DDE-BIFTOOL. Among other things, we find stable small-amplitude solutions outside the region of linear stability of the pendulum, which can be interpreted as a relaxed form of successful control.

Submitted to: *Nonlinearity*

AMS classification scheme numbers: 34K17, 34K35, 37G10, 37G40

1. Introduction

Many applications give rise to dynamical systems that do not only depend on their present state, but also on their state at some time τ ago. One speaks of systems with delay, and τ is called the delay time. Examples are lasers subject to optical feedback due to external reflections [22], coupled neurons [25, 30], and milling tools that encounter their own effect on the workpiece one milling cycle ago [27]. Another important field where delays arise is control theory [26]. After all, it is not possible to react to the state of a dynamical system instantaneously, so that any control action will take effect only after a fixed delay, given by a reaction time. In some situations this delay may be so small as to be negligible, but often it is large enough to have a significant influence on

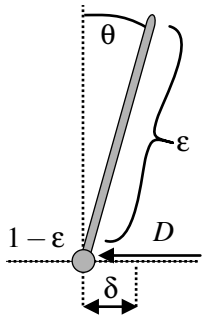

Figure 1. Sketch of the inverted pendulum on a cart.

the overall dynamics of the controlled system. A classic example is the known fact that it is easier for a human being to balance a longer rather than a shorter stick [31]. Making the stick shorter effectively increases the reaction time, up to a point that balancing the stick becomes impossible. (The reaction time can be increased directly, for example, by the consumption of alcohol, which leads to other known detrimental effects on the subject's ability to assert effective balancing control.)

In this paper we consider a classic control problem: an inverted planar pendulum on a motorized cart on a track. The goal of the feedback controller is to control the pendulum in the upright position, where the control action is the movement of the cart; see figure 1. This system is the standard example of a nonlinear oscillator that is controlled to an unstable equilibrium [7] and, at the same time, a prototype for balancing problems occurring in robotics and biomechanics [5, 15].

To study the influence of delay on the dynamics of the controlled pendulum, we consider a simple case of a linear feedback controller; introduced in section 2 below. The equations of motion are then given as a delay differential equation (DDE) with a two-dimensional physical space, the space of (angular) displacement and velocity of the pendulum. The class of DDEs is quite difficult to study because a DDE has an infinite-dimensional phase space, the space of continuous functions over the delay interval $[-\tau, 0]$; see Refs. [9, 18] as general references to the theory of DDEs. (We consider here only the case of a single fixed delay, but theory is available for any number of fixed delays and for certain classes of state-dependent or distributed delays.) It is an important property of DDEs with one fixed delay that the linearized operators at equilibria and around periodic orbits, respectively, have no essential spectrum and their characteristic roots are isolated (except at 0 in the case of periodic orbits). Furthermore, there can be at most finitely many unstable eigenvalues of an equilibrium and Floquet multipliers of a periodic orbit. Consequently, the local bifurcation theory of equilibria and periodic orbits follows that of ordinary differential equations (ODEs). In particular, it is possible to compute normal forms on suitable center manifolds [6], but this is a lot more involved for DDEs than for ODEs.

Starting from the linear stability analysis of the inverted pendulum on a cart with delayed linear control, we identify as an organizing center a codimension-three

singularity where the origin has a triple-zero eigenvalue. The unfolding of this singularity in the generic case is the topic of Refs. [11, 12, 14]. However, in the words of Ref. [12], 'the bifurcation diagram is very complicated and a complete study is far beyond the current possibilities.' Furthermore, the system we are considering has an extra $\mathbb{Z}_2$-symmetry. We construct the expansion of the three-dimensional center manifold of the DDE near this singularity and derive the vector field

$$\begin{aligned} \dot{u}_1 &= u_2 \\ \dot{u}_2 &= u_3 \\ \dot{u}_3 &= -\alpha u_1 + \gamma u_2 + \beta u_3 + u_1^3 \end{aligned} \tag{1}$$

describing the dynamics of the three-jet on the center manifold. We use that (1) has cone structure to reduce the bifurcation analysis to a sphere around the central singularity, where we perform the relevant linear stability analysis and compute global bifurcations numerically with the continuation software AUTO [10]. While the study of a complete unfolding of a triple-zero singularity with $\mathbb{Z}_2$-symmetry is beyond the scope of this paper, our analysis of (1) provides at least a partial unfolding. Specifically, we find numerical evidence that (1) is conservative for a certain choice of parameters, so that the full unfolding of the $\mathbb{Z}_2$-symmetry triple-zero singularity must include other terms.

We remark that a recent study of Chua's circuit with a cubic nonlinearity in Ref. [1] also found a triple-zero singularity with the same $\mathbb{Z}_2$-symmetry (due to the symmetry of the three-dimensional Chua equations) as an organizing center. The ODE (1) was found independently in Ref. [1] as a truncated normal form near the singularity, but it was not studied as a possible unfolding. Instead these authors concentrated on a detailed analysis of local and global bifurcations in the Chua equations themselves, where they found that other codimension-three bifurcations add to the overall complexity of bifurcations.

Our approach here is to obtain a complete description of the family of symmetric periodic orbits (including its bifurcations) that is emerging from the origin at the singularity. As one part of this family of symmetric periodic orbits is stable, our results show that it is not possible to reduce the pendulum model to its linearization (neglecting the geometric nonlinearity as in Ref. [21]) in the presence of a delay, even though we consider only small-amplitude dynamics and linear feedback.

The question of how the results of the partial unfolding manifest themselves in the DDE is addressed by computing the bifurcation diagram in the DDE near the triple-zero singularity directly with the recently developed continuation software DDE-BIFTOOL [13]. As a result we can conclude that the singularity indeed acts as an organizing center in quite a large region of the parameter space of the original DDE.

The paper is organized as follows. We first give details of the mathematical model in section 2 and then recall its linear stability in section 3. Next we compute the center manifold of the triple-zero singularity and the ODE governing the flow on it in section 4. section 5 presents the bifurcation analysis of the reduced model, constituting a partial unfolding of the triple-zero singularity in the presence of $\mathbb{Z}_2$-symmetry. How the bifurcation set of the reduced model is embedded in the full DDE is studied in

section 6. Finally, we draw conclusions and discuss open problems in section 7.

2. Mathematical model

In dimensionless form, the dynamics of the inverted pendulum on a cart in figure 1 are governed by the second-order differential equation for θ:

$$\left(1 - \frac{3\varepsilon}{4}\cos^2\theta\right)\ddot{\theta} + \frac{3\varepsilon}{8}\dot{\theta}^2\sin(2\theta) - (\sin\theta + D\cos\theta) = 0. \tag{2}$$

Here $\varepsilon = m/(m+M)$ is the relative mass of the pendulum, where m is the mass of the uniform pendulum and M is the mass of the cart, and D is the horizontal driving force rescaled by $(m+M)g$. Time has been rescaled by $\sqrt{2L/(3g)}$, where L is the length of the pendulum and g is the constant of gravity.

The displacement δ of the cart depends on θ via the odd function

$$\delta(t) = L\int_0^t\int_0^s \frac{\frac{\varepsilon}{2}\sin\theta\dot{\theta}^2 + \frac{2}{3}D - \frac{\varepsilon}{4}\sin(2\theta)}{1 - \frac{3\varepsilon}{4}\cos^2\theta}\,ds\,dt \tag{3}$$

if we assume that $\delta(0) = \dot{\delta}(0) = 0$. The force D is applied as a feedback control depending on the state of the system with the goal of stabilizing the pendulum at its upright position, $\theta = 0$.

Due to inherent delays, the feedback control force D is a function of the state of the system at some fixed time τ ago. We do not assume this delay to be negligible, but consider its influence on the dynamics of the overall system. To this end, we study the case of a linear control force

$$D(t) = -a\theta(t-\tau) - b\dot{\theta}(t-\tau) \tag{4}$$

with the single fixed delay time $\tau \geq 0$ in the controller, and the control gains a and b. We remark that increasing the delay time τ corresponds to decreasing the length L of the pendulum.

Equation (2) can be written as a delay differential equation (DDE) of the form

$$\dot{x}(t) = f(x(t), x(t-\tau), \lambda) \tag{5}$$

which relates to (2) and (4) by setting $x_1 = \theta$, $x_2 = \dot{\theta}$ and $\lambda = (a, b, \tau)$. The right-hand-side $f : \mathbb{R}^2 \times \mathbb{R}^2 \times \mathbb{R}^3 \to \mathbb{R}^2$ has the form

$$\begin{aligned} f_1(x, y, \lambda) &= x_2 \\ f_2(x, y, \lambda) &= \frac{-\frac{3}{8}\varepsilon\sin(2x_1)x_2^2 + \sin x_1 - \cos x_1(ay_1 + by_2)}{1 - \frac{3}{4}\varepsilon\cos^2 x_1}. \end{aligned} \tag{6}$$

The phase space of (5)–(6) is the space of continuous functions over the delay interval $[-\tau, 0]$ with values in $\mathbb{R}^2$. The two-dimensional (x_1, x_2)-space is called the physical space $\mathbb{R}^2$.

System (5)–(6) has $\mathbb{Z}_2$-symmetry, because the function f is odd, that is,

$$f(-x, -y, \lambda) = -f(x, y, \lambda). \tag{7}$$

Consequently, the origin 0 is always an equilibrium, and any solution of (5)–(6) is either symmetric under this symmetry or has a counterpart under reflection at the origin.

The target of the controller is to balance the system shown in figure 1 at its upright position, the origin of (5)–(6). In the case of perfect control the displacement $\delta(t)$ has a constant velocity as the system reaches the origin, which is then a stable symmetric attractor, as is shown in figure 2(a). (Note that in this case we can ensure that $\delta(t) \to 0$ and $\dot{\delta}(t) \to 0$ for $t \to \infty$ by choosing appropriate initial conditions for δ and $\dot{\delta}$.) We relax the notion of successful control somewhat: we speak of successful control if $\dot{\delta}(t)$ remains bounded along the trajectory $x(t)$. This is the case only when the system reaches a stable symmetric state, such as an equilibrium (the case of perfect control), a symmetric periodic orbit, or a more complicated symmetric invariant set. In other words, we allow the pendulum to show some (ideally small) motion around its upright position, as in figure 2(b). A non-symmetric attractor, on the other hand, corresponds to the pendulum leaning to one side, which has to be compensated by an acceleration of the displacement $\delta(t)$, in other words $\dot{\delta}(t)$ is not bounded; see figure 2(c).

3. Linear stability analysis at the origin

The linear stability of (5)–(6) at the origin has been analyzed already in Ref. [31]. We recall these results because they allow us to identify a codimension-three singularity, where the origin has a triple-zero eigenvalue, as the organizing center of small-amplitude dynamics; see figure 3 for illustration.

The linearizations of f with respect to its two arguments x and y at the origin are

$$\partial_1 f(0,0,\lambda) = \begin{bmatrix} 0 & 1 \\ \frac{4}{4-3\varepsilon} & 0 \end{bmatrix} \qquad \text{and} \qquad \partial_2 f(0,0,\lambda) = \begin{bmatrix} 0 & 0 \\ -\frac{4a}{4-3\varepsilon} & -\frac{4b}{4-3\varepsilon} \end{bmatrix}.$$

Hence, the characteristic function of the linearization

$$\dot{x}(t) = \partial_1 f(0,0,\lambda)x(t) + \partial_2 f(0,0,\lambda)x(t-\tau) \tag{8}$$

of system (5) at the origin is given by

$$\begin{aligned} \chi(\zeta) &= \det\left[\zeta I - \partial_1 f(0,0,\lambda) - \partial_2 f(0,0,\lambda)e^{-\tau\zeta}\right] \\ &= \zeta^2 - \frac{4}{4-3\varepsilon}\left(1 - e^{-\tau\zeta}(\zeta b + a)\right). \end{aligned}$$

The function χ has a root 0 along the solid curve in figure 3, given by $\{a = 1\}$, where the origin undergoes a pitchfork bifurcation (the generic bifurcation in light of the symmetry (7)). A pair of equilibria, given by $\tan x_1 = a x_1$ and $x_2 = 0$, emerges from 0 for $a > 1$. The function χ has a purely imaginary root $i\omega$ ($\omega \in \mathbb{R}$) if

$$\begin{aligned} a &= \cos(\omega\tau)\left[\omega^2\left(1 - \frac{3}{4}\varepsilon\right) + 1\right], \\ b &= \frac{\sin(\omega\tau)}{\omega}\left[\omega^2\left(1 - \frac{3}{4}\varepsilon\right) + 1\right]. \end{aligned} \tag{9}$$

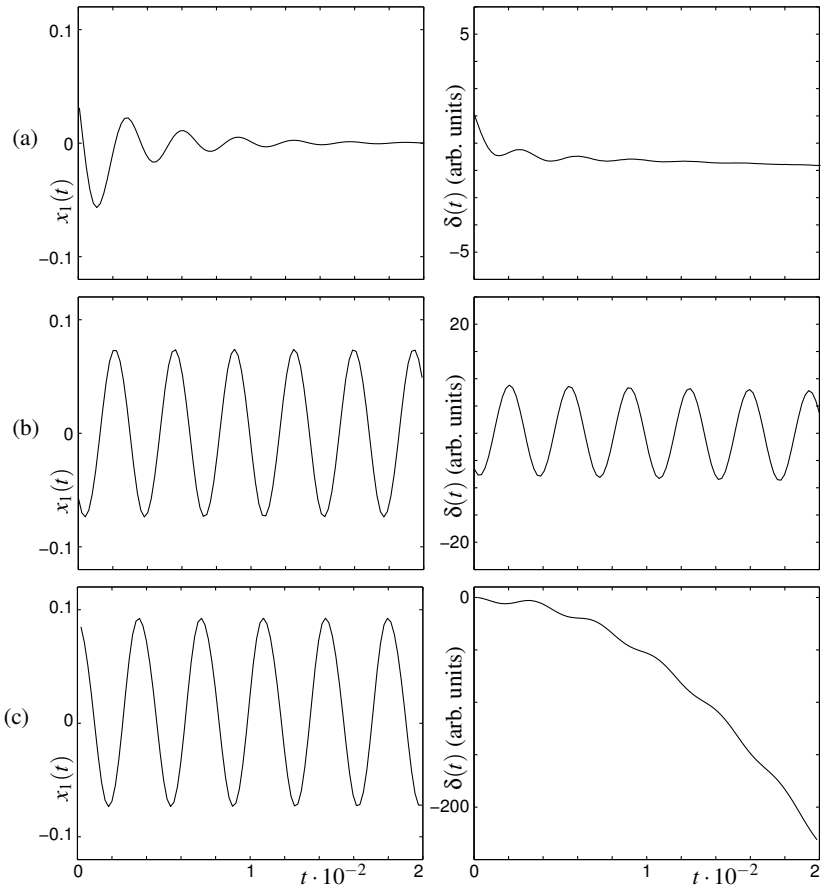

Figure 2. Time profile of the angle x_1 (left column) and the displacement of the cart δ (right column) for the case of perfect stabilization constant cart velocity (a), stabilization with bounded car velocity (b), and an example of accelerating cart motion (c). (The panels correspond to the indicated parameter points in figure 8, namely from (a) to (c) φ takes the values 0.2, 0.4 and 0.435 and $\psi = 0.65$ throughout.)

Equations (9) define the curve of Hopf bifurcations in the (a, b)-plane (dashed line in figure 3), which can be parametrized by $\omega \in [0, \infty)$. This curve originates for $\omega = 0$ from the point DZ, given by $(a, b) = (1, \tau)$, where the origin has an eigenvalue 0 of algebraic multiplicity two and geometric multiplicity one. Our model (5)-(6) has a two-dimensional center manifold for parameters near DZ. The flow on this manifold is governed by a $\mathbb{Z}_2$-symmetric planar vector field. The dynamics near the *double-zero singularity* DZ correspond to those of the normal form vector field approximation of the 1:2 resonance for maps — a classic bifurcation that can be found, for example, in Ref. [24].

For $\tau = 0$, the Hopf curve is the ray $\{a > 1, b = 0\}$. The origin is stable in the region $\{b > 0, a > 1\}$, it has one unstable direction in $\{a < 1\}$, and two unstable directions in $\{b < 0, a > 1\}$. At $b = 0$ the system is a two-dimensional conservative oscillator conserving the quantity $(1 - \frac{3}{4}\varepsilon \cos^2 x_1)x_2^2/2 + (1+a)\cos x_1 + a x_1 \sin x_1$. Hence, the Hopf bifurcation is degenerate for $\tau = 0$. The global bifurcations of the periodic

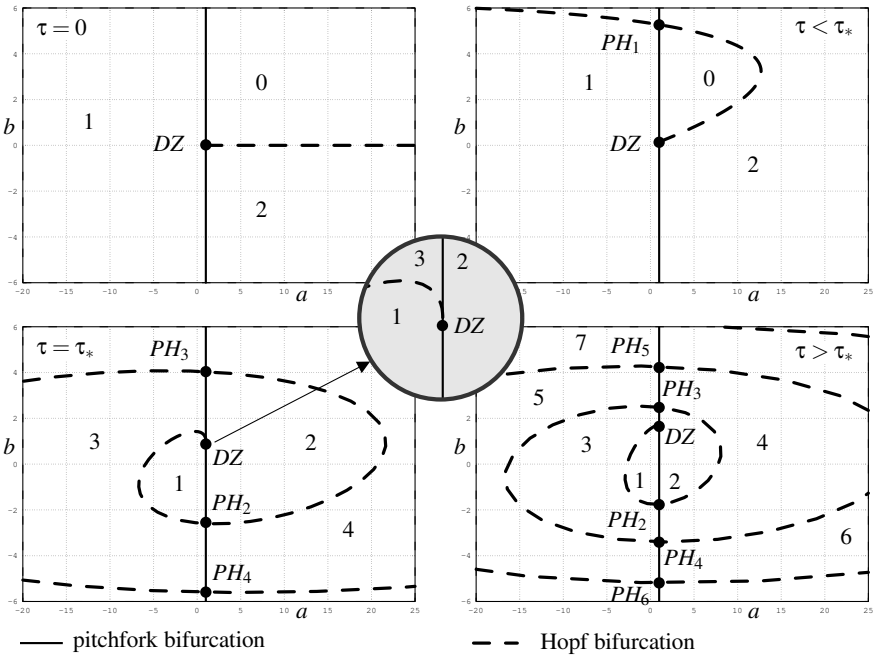

Figure 3. Linear stability at the origin of (5)–(6) in the (a, b)-plane for $\varepsilon = 2/3$ and $\tau = 0.0,\ 0.15,\ 1.0,\ 1.7$. Shown are the pitchfork (solid) and Hopf (dashed) bifurcation curves; the number of unstable eigenvalues of the origin is indicated for each region; the inset is an enlargement near the triple-zero eigenvalue degeneracy.

orbits will be studied in section 5.

For positive τ, the Hopf curve spirals outward in a counterclockwise fashion asymptotically for large ω. Apart from DZ, all intersections PH_j of the Hopf curve with the pitchfork line are pitchfork-Hopf interactions with one zero eigenvalue and (generically) one complex conjugate pair of eigenvalues for some imaginary part $\pm i\omega$ with $\omega > 0$.

The derivative $da/d\omega$ of the Hopf curve at $\omega = 0$ (that is, at the point DZ) is given by

$$\left.\frac{da}{d\omega}\right|_{\omega=0} = 2 - \frac{3}{2}\varepsilon - \tau^2.$$

Hence, there exists a region of linear stability of the origin in the (a, b)-plane to the upper right of DZ provided τ is small enough, more precisely, if

$$\tau < \tau_* := \frac{1}{2}\sqrt{8 - 6\varepsilon}. \tag{10}$$

The region of stability is bounded on the left by the pitchfork line $\{a = 1\}$ and on the right by the Hopf curve, both between DZ and PH_1, the first intersection of the Hopf and the pitchfork curve. This bounded region shrinks for increasing τ and it disappears at $\tau = \tau_*$; see (10). At $\tau = \tau_*$ the points DZ and PH_1 coincide. Hence, the linearization at the origin has an eigenvalue 0 of algebraic multiplicity three and of geometric multiplicity one. This codimension-three singularity occurs at

$(a, b, \tau) = (1, \tau_*, \tau_*)$ and it acts as an organizing center of the dynamics. One speaks of a *non-semisimple triple-zero eigenvalue* or the *nilpotent singularity of codimension three* [11, 14]. Due to the symmetry of the equations, we are not dealing with the generic case, but with a $\mathbb{Z}_2$-symmetric triple zero eigenvalue singularity, which one might interpret as a pitchfork-Hopf interaction with an additional degenerate direction. In the following sections we investigate the small-amplitude dynamics of (5) in the vicinity of this triple-zero singularity.

Finally, there cannot be any stable small-amplitude motion for $\tau > \tau_*$ because the origin has a strongly unstable eigenvalue for all $a > 0$ and $b > 0$.

4. Center manifold reduction near the triple-zero singularity

For DDEs, there are well-established results about the existence and properties of local center manifolds close to equilibria with critical eigenvalues; see, for example, Ref. [9]. In order to be able to apply the results of Ref. [9] for a reduction of our model (5)-(6) we take three steps. First, we reformulate (5)-(6) as an evolution equation in a Banach space. Second, we compute the invariant subspaces of the linearization at the triple-zero singularity and the corresponding invariant projections. In the third step, we zoom into the neighborhood of the singularity (in parameter space and phase space) by introducing a small parameter r as a scaling parameter, and expand the nonlinearity in powers of r. In this way, we derive an expansion of the flow on the center manifold in r. Finally, the truncation of all terms of higher order in r leads to the reduced model. Most calculations in this section are technical but straightforward if one uses computer algebra systems; we used Maple [8]. Readers which are not interested in the details of this procedure may skip directly to Theorem 2 at the end of this section, which introduces the truncated reduced model and shows how its dynamics are related to the dynamics of the original model (5)-(6).

4.1. Corresponding evolution equation

Since we investigate the neighborhood of the parameter point

$$\lambda_0 = (a_0, b_0, \tau_0) = (1, \tau_*, \tau_*),$$

the delay τ is uniformly positive. Hence, we can rescale time such that the delay is equal to 1. After this transformation and a rescaling of $\dot{x}$, the DDE has the form

$$\dot{x}(t) = \tilde{f}(x(t), x(t-1), \lambda) \tag{11}$$

where $\tilde{f} : \mathbb{R}^2 \times \mathbb{R}^2 \times \mathbb{R}^3 \to \mathbb{R}^2$ is

$$\begin{aligned} \tilde{f}_1(x, y, \lambda) &= x_2 \\ \tilde{f}_2(x, y, \lambda) &= \frac{-\frac{3}{8}\varepsilon \sin(2x_1)x_2^2 + \tau^2 \sin x_1 - \cos x_1(\tau^2 a y_1 + \tau b y_2)}{1 - \frac{3}{4}\varepsilon \cos^2 x_1}. \end{aligned} \tag{12}$$

For notational convenience, and because we will consider only the rescaled model from now on, we drop the tilde and denote the right-hand side of (11)-(12) simply by f.

We denote the Banach space of continuous functions on the interval $[-1,0]$ into $\mathbb{R}^2$ by $C([-1,0];\mathbb{R}^2)$, and the space of k times continuously differentiable functions by $C^k([-1,0];\mathbb{R}^2)$. Let X be the Banach space $\mathbb{R}^2 \times C([-1,0];\mathbb{R}^2)$. We define the linear operator $H : D(H) \subset X \to X$ on

$$D(H) := \{(y,\tilde{y}) \in \mathbb{R}^2 \times C^1([-1,0];\mathbb{R}^2) : \tilde{y}(0) = y\} \subset X$$

by

$$H \begin{bmatrix} y \\ \tilde{y} \end{bmatrix} = \begin{bmatrix} A\tilde{y}(0) + B\tilde{y}(-1) \\ \partial_s \tilde{y} \end{bmatrix}$$

where the spatial variable in $C^1([-1,0];\mathbb{R}^2)$ is denoted by s, and

$$A = \partial_1 f(0,0,\lambda_0) = \begin{bmatrix} 0 & 1 \\ 2 & 0 \end{bmatrix}, \qquad B = \partial_2 f(0,0,\lambda_0) = \begin{bmatrix} 0 & 0 \\ -2 & -2 \end{bmatrix}$$

are the linearizations of f in the origin at λ_0. The linear operator H is a closed unbounded operator. It generates a semigroup $T(t) : X \to X$ of bounded operators. The semigroup $T(\cdot)$ is not strongly continuous since $D(H)$ is not dense in X, but $T(\cdot)$ is compact for $t > 1$; see Ref. [28] for details.

We define the nonlinearity $g \in C^\infty(X \times \mathbb{R}^3; X)$ by

$$\begin{aligned} g\left(\begin{bmatrix} y \\ \tilde{y} \end{bmatrix}, \lambda\right) &= \begin{bmatrix} g_0(\tilde{y}(0), \tilde{y}(-1), \lambda) \\ 0 \end{bmatrix} \quad \text{where} \\ g_0(\tilde{y}(0), \tilde{y}(-1), \lambda) &= f(\tilde{y}(0), \tilde{y}(-1), \lambda) - A\,\tilde{y}(0) - B\,\tilde{y}(-1). \end{aligned} \tag{13}$$

System (11)-(12) is equivalent to the autonomous evolution equation

$$\dot{x} = Hx + g(x,\lambda), \tag{14}$$

and $\|g(x,\lambda)\|$ is of order $O(\|(x,\lambda-\lambda_0)\|^2)$ in X. The linear part $\dot{x} = Hx$ is equivalent to the linearization of (11)-(12) at the singularity. Consequently, H has an eigenvalue 0 of algebraic multiplicity three and geometric multiplicity one.

4.2. H-invariant decomposition of X

In the next step, we decompose the Banach space X into a direct sum

$$X = \mathcal{N} \oplus \mathcal{H}$$

of H-invariant subspaces. The subspace $\mathcal{N}$ is the generalized nullspace of H. It is isomorphic to $\mathbb{R}^3$ since the eigenvalue 0 has algebraic multiplicity three. The semigroup $T(t)$ restricted to H decays exponentially with some rate $\rho > 0$ according to Ref. [9]:

$$\|T(t)x\| \le Ce^{-\rho t}\|x\| \quad \text{for all } x \in \mathcal{H}. \tag{15}$$

Let us decompose (14) into an ODE in $\mathbb{R}^3$ and an evolution equation in H. We choose $\mathcal{B} = [b_1, b_2, b_3]$ as the basis of $\mathcal{N}$ such that $H\,\mathcal{B} = \mathcal{B}\,J$ where

$$b_1 = \begin{bmatrix} 1 \\ 0 \\ 1 \\ 0 \end{bmatrix}, \qquad b_2 = \begin{bmatrix} 0 \\ 1 \\ s \\ 1 \end{bmatrix}, \qquad b_3 = \begin{bmatrix} 1 \\ 0 \\ 1 + \frac{1}{2}s^2 \\ s \end{bmatrix}, \quad \text{and} \quad J = \begin{bmatrix} 0 & 1 & 0 \\ 0 & 0 & 1 \\ 0 & 0 & 0 \end{bmatrix}.$$

The invariant projection $P : X \to \mathcal{N}$ onto $\mathcal{N}$ is defined by the integral $Px = \mathrm{Res}_{z=0}\,(zI - H)^{-1}$; see Ref. [20]. It has the form $Px = l_1[x]\,b_1 + l_2[x]\,b_2 + l_3[x]\,b_3$ where

$$
\begin{aligned}
l_1 \begin{bmatrix} y \\ \tilde{y} \end{bmatrix} &= -\frac{621}{320}y_1 - \frac{921}{640}y_2 + \int_{-1}^{0} \left[\frac{801}{320} - \frac{15}{8}s - \frac{3}{2}s^2\right] (\tilde{y}_1(s) + \tilde{y}_2(s))\,ds, \\
l_2 \begin{bmatrix} y \\ \tilde{y} \end{bmatrix} &= -\frac{3}{8}y_1 + \frac{9}{16}y_2 + \int_{-1}^{0} \left[\frac{15}{8} + 3s\right] (\tilde{y}_1(s) + \tilde{y}_2(s))\,ds, \\
l_3 \begin{bmatrix} y \\ \tilde{y} \end{bmatrix} &= 3y_1 + \frac{3}{2}y_2 - \int_{-1}^{0} 3\tilde{y}_1(s) + 3\tilde{y}_2(s)\,ds.
\end{aligned}
$$

We decompose (14) using the projections $\mathcal{B}^{-1}P = [l_1, l_2, l_3]^T$: $X \to \mathbb{R}^3$ and $I - P$, and define

$$
\begin{aligned}
P_0 &= \mathcal{B}^{-1}P \begin{bmatrix} 1 & 0 \\ 0 & 1 \\ 0 & 0 \\ 0 & 0 \end{bmatrix} = \begin{bmatrix} -\frac{621}{320} & -\frac{921}{640} \\ -\frac{3}{8} & \frac{9}{16} \\ 3 & 3 \end{bmatrix}, \\
\tilde{\mathcal{B}} &= \begin{bmatrix} 0 & 0 & 1 & 0 \\ 0 & 0 & 0 & 1 \end{bmatrix} \mathcal{B} = \begin{bmatrix} 1 & s & 1 + \frac{1}{2}s^2 \\ 0 & 1 & s \end{bmatrix}, \\
D_0 = \tilde{\mathcal{B}}|_{s=0} &= \begin{bmatrix} 1 & 0 & 1 \\ 0 & 1 & 0 \end{bmatrix}, \\
D_1 = \tilde{\mathcal{B}}|_{s=-1} &= \begin{bmatrix} 1 & -1 & \frac{3}{2} \\ 0 & 1 & -1 \end{bmatrix}.
\end{aligned}
$$

Then the decomposed system for $x = \mathcal{B}v + w$ ($v \in \mathbb{R}^3$, $w = (w_0, \tilde{w})^T \in \mathcal{H}$ where $w_0 \in \mathbb{R}^2$, $\tilde{w} \in C([-1, 0]; \mathbb{R}^2)$ reads as follows:

$$
\begin{aligned}
\dot{v} &= Jv + P_0\, g_0(D_0 v + \tilde{w}(0), D_1 v + \tilde{w}(-1), \lambda), \\
\dot{w}_0 &= A\tilde{w}(0) + B\tilde{w}(-1) + (I - D_0 P_0)\, g_0(D_0 v + \tilde{w}(0), D_1 v + \tilde{w}(-1), \lambda), \\
\dot{\tilde{w}} &= \partial_s \tilde{w} - \tilde{\mathcal{B}}\, P_0\, g_0(D_0 v + \tilde{w}(0), D_1 v + \tilde{w}(-1), \lambda),
\end{aligned}
\tag{16}
$$

where $\tilde{w}(0) = w_0$.

If we denote the semiflow generated by (16) by $\mathcal{S}(t; v, w, \lambda)$ then $\mathcal{S}$ is equivalent to the semiflow generated by (14). The local center manifold theorem of Ref. [9, Chapter IX, pp. 259–286] implies the existence of a center manifold for system (16):

Theorem 1 (Existence and properties of the center manifold)
Let $k > 0$, and $\mathcal{U}_v \times \mathcal{U}_w \times \mathcal{U}_p$ be a sufficiently small neighborhood of $(0, 0, \lambda_0)$ in $\mathbb{R}^3 \times \mathcal{H} \times \mathbb{R}^3$. There exists a graph $\omega : \mathcal{U}_v \times \mathcal{U}_p \to \mathcal{H}$ of smoothness C^k such that the following statements hold.

(i) (Invariance) *The manifold $\{(v, w) \in \mathcal{U}_v \times \mathcal{H} : w = \omega(v, \lambda)\}$ is invariant with respect to $\mathcal{S}$ relative to $\mathcal{U}_v \times \mathcal{U}_w$.*

(ii) (Exponential Attraction) *Let* (v, w) *be such that* $\mathcal{S}(t; v, w, \lambda) \in \mathcal{U}_v \times \mathcal{U}_w$ *for all* $t \geq 0$. *Then, there exist* $\hat{v} \in \mathcal{U}_v$ *and* $\hat{t} \geq 0$ *such that*

$$\|\mathcal{S}(t + \hat{t}; v, w, \lambda) - \mathcal{S}(t; \hat{v}, \omega(\hat{v}), \lambda)\| \leq Ce^{-t\rho/2} \quad \textit{for all } t > 0.$$

The second statement says that all interesting dynamics in the neighborhood of the origin happens on the center manifold.

4.3. Expansion of the center manifold

In the next step, we zoom into the neighborhood of the singularity by introducing a small parameter r as the scaling parameter. Then we expand the nonlinearity g_0 of the decomposed system (16), which has been defined in (13), and the graph ω from Theorem 1 in powers of r.

We introduce the following change of variables:

$$\begin{aligned} v &= r^3 \begin{bmatrix} 1 & 0 & 0 \\ 0 & r^2 & 0 \\ 0 & 0 & r^4 \end{bmatrix} u, \\ w &= r^3 z, \\ a &= 1 + \alpha \frac{1}{3} r^6, \\ b &= \tau_* + \beta \frac{\tau_*}{3} r^2, \\ \tau &= b + \gamma \frac{\tau_*}{3} r^4, \\ t_{\text{old}} &= r^2 t_{\text{new}}. \end{aligned} \tag{17}$$

The new parameter vector $\mu = (\alpha, \beta, \gamma)$ measures the distance of the parameter λ to λ_0. We denote the two components of the non-central variable z by z_0 and $\tilde{z}$ (where $z_0 \in \mathbb{R}^2$, $\tilde{z} \in C([-1, 0]; \mathbb{R}^2)$ and insert the scaled variables defined in (17) as arguments into the nonlinearity g_0 of the decomposed system (16). We denote the nonlinearity obtained by this insertion by h:

$$g_0(D_0 v + \tilde{w}(0), D_1 v + \tilde{w}(-1), \lambda) =: h(u, \tilde{z}(0), \tilde{z}(-1), \mu, r) \quad \text{using (17)}.$$

The two components of h have expansions of the following structure:

$$\begin{aligned} h_1(u, \tilde{z}(0), \tilde{z}(-1), \mu, r) &= 0 \\ h_2(u, \tilde{z}(0), \tilde{z}(-1), \mu, r) &= r^5 \eta_5(\mu)[\tilde{z}(0), \tilde{z}(-1)] + r^7 \eta_7(\mu)[\tilde{z}(0), \tilde{z}(-1)] \\ &\quad + r^9 \eta_9(u, \tilde{z}(0), \tilde{z}(-1), \mu) + r^{11} \eta_{11}(u, \tilde{z}(0), \tilde{z}(-1), \mu, r). \end{aligned} \tag{18}$$

We observe that the first non-zero coefficient of the expansion of h_2 corresponds to r^5. Moreover, η_5 and η_7 do not depend on u and are linear in z. Consequently, the evolution

equation for $z \in \mathcal{H}$ has the following structure

$$\begin{aligned} r^2\dot{z} = \; & Hz + r^{-3} \begin{bmatrix} I - D_0 P_0 \\ -\tilde{\mathcal{B}} P_0 \end{bmatrix} \begin{bmatrix} 0 \\ 1 \\ 0 \\ 1 \end{bmatrix} h_2(u, \tilde{z}(0), \tilde{z}(-1), \mu) \\ = \; & Hz + C \cdot \big(r^2 \eta_5(\mu)[\tilde{z}(0), \tilde{z}(-1)] + r^4 \eta_7(\mu)[\tilde{z}(0), \tilde{z}(-1)] \\ & + r^6 \eta_9(u, \tilde{z}(0), \tilde{z}(-1), \mu) + O(r^8) \big) . \end{aligned} \tag{19}$$

According to (15), the semigroup T generated by H decays with rate ρ in the subspace $\mathcal{H}$. The center manifold is a graph representing z as a function of u, μ and r. Expansion (19) implies that the expansion of this graph in powers of r is of order r^6, that is,

$$z(u, \mu, r) = r^6 z_6(u, \mu, r). \tag{20}$$

We insert the expansion (20) of the graph of the center manifold for z in the nonlinearity h_2 to obtain an expansion in r of the flow on the center manifold (where we denote the $C([-1, 0]; \mathbb{R}^2)$ component of the graph $z(u, \mu, r)$ by $\tilde{z}(u, \mu, r)$):

$$\begin{aligned} h_2(u, \tilde{z}(u, \mu, r)(0), \tilde{z}(u, \mu, r)(-1), \mu, r) &= r^9 \eta_9(u, 0, 0, \mu) + O(r^{11}), \\ &= r^9 \, \frac{2}{3} \left(-\alpha \, u_1 + \gamma \, u_2 + \beta \, u_3 + u_1^3 \right) + O(r^{11}). \end{aligned}$$

Consequently, the flow on the local center manifold of (14) is governed by the system of ODEs

$$\begin{aligned} \dot{u} &= Ju + r^{-5} \begin{bmatrix} 1 & 0 & 0 \\ 0 & r^{-2} & 0 \\ 0 & 0 & r^{-4} \end{bmatrix} P_0 h_2(u, \tilde{z}(u, \mu, r)(0), \tilde{z}(u, \mu, r)(-1), \mu, r) \\ &= \begin{bmatrix} 0 & 1 & 0 \\ 0 & 0 & 1 \\ -\alpha & \gamma & \beta \end{bmatrix} u + \begin{bmatrix} 0 \\ 0 \\ u_1^3 \end{bmatrix} + r^2 R(u, \mu, r) \end{aligned} \tag{21}$$

where the remainder $R : \mathbb{R}^3 \times \mathbb{R}^3 \times \mathbb{R} \to \mathbb{R}^3$ is a smooth function in u, $\mu = (\alpha, \beta, \gamma)$, and r. Regular perturbation theory [19] implies the following result:

Theorem 2 (Truncated reduced model) *Let $\mathcal{M}$ be a manifold of dimension less than three with an embedding $\hat{u} : \mathcal{M} \to \mathbb{R}^3$. Let $\hat{u}(\mathcal{M})$ be a normally hyperbolic invariant manifold of the system of ODEs*

$$\begin{pmatrix} \dot{u}_1 \\ \dot{u}_2 \\ \dot{u}_3 \end{pmatrix} = \begin{pmatrix} 0 & 1 & 0 \\ 0 & 0 & 1 \\ -\alpha & \gamma & \beta \end{pmatrix} \begin{pmatrix} u_1 \\ u_2 \\ u_3 \end{pmatrix} + \begin{pmatrix} 0 \\ 0 \\ u_1^3 \end{pmatrix} . \tag{22}$$

Then, there exist an upper bound $r_0 > 0$ and a family of embeddings $\hat{x} : (0, r_0) \times \mathcal{M} \to X$ for which the following statements hold:

(i) $\hat{x}$ is continuous with respect to $r \in (0, r_0)$,

(ii) $\hat{x}(r, \mathcal{M})$ *is a normally hyperbolic invariant manifold of the evolution equation (14) with the parameters*

$$a = 1 + r^6\alpha, \qquad b = \tau_* + \beta\,\frac{\tau_*}{3}r^2, \qquad \tau = \; b + \gamma\,\frac{\tau_*}{3}r^4, \tag{23}$$

(iii) the approximation $\hat{x}(r, m) = r^3\hat{u}_1(m)b_1 + O(r^5)$ *holds for all* $m \in \mathcal{M}$*, and*

(iv) if $\hat{u}(\mathcal{M})$ *is stable for (22), then* $\hat{x}(r, \mathcal{M})$ *is stable for the evolution equation (14) with the parameter set of (23).*

Special cases of normally hyperbolic invariant manifolds are equilibria without eigenvalues on the imaginary axis ($\mathcal{M} = \{0\}$), and periodic orbits without Floquet multipliers of modulus 1 ($\mathcal{M} = S^1$). Theorem 2 provides a direct interpretation of the orbits found in the reduced model (22) in terms of the original physical quantities of the DDE (11)-(12): if $u(t)$ is a normally hyperbolic periodic orbit of (22), there exists a normally hyperbolic periodic orbit in (11)-(12) satisfying $x_1(t) = r^3u_1(r^2t) + O(r^5)$.

Notice that the mass ratio ε affects only the location of the singularity λ_0 and the scaling but does not enter the coefficients of the nonlinear terms of order one in (22). Finally, we remark that the $\mathbb{Z}_2$-symmetry of (22) is given by the symmetry operation $(u_1, u_2, u_3) \to (-u_1, -u_2, -u_3)$. (This is the same symmetry as that of the Chua equations studied in Ref. [1].)

5. Bifurcation analysis of the reduced model

Theorem 2 implies that (22) is a partial unfolding of the non-semisimple triple-zero eigenvalue bifurcation in the presence of the $\mathbb{Z}_2$-symmetry given by (7). The unfolding is complete at the linear level, that is, any small perturbation of the matrix J can be transformed into the form

$$\begin{pmatrix} 0 & 1 & 0 \\ 0 & 0 & 1 \\ -\alpha & \gamma & \beta \end{pmatrix}$$

by a linear near-identity transformation. A notable difference between (22) and the normal forms derived in Refs. [12, 14] is the absence of affine and quadratic terms due to the $\mathbb{Z}_2$-symmetry; see also [1].

We now summarize the linear stability analysis of the origin of (22).

Lemma 3 *The origin is stable for* $\beta < 0$, $\gamma < 0$, *and* $0 < \alpha < \beta\gamma$. *It changes its stability as follows:*

(i) The origin undergoes a pitchfork bifurcation at $\alpha = 0$. *For* $\alpha > 0$, *there are two equilibria at* $u = (\pm\sqrt{\alpha}, 0, 0)$.

(ii) The origin undergoes a Hopf bifurcation at $\alpha = \beta\gamma$ *for* $\gamma \leq 0$.

The following local codimension-2 bifurcations occur:

(i) The origin has a double-zero singularity for $\alpha = \gamma = 0$, *that is, the linearization at the origin has a double eigenvalue* 0 *and a third eigenvalue* β.

(ii) The origin has a pitchfork-Hopf interaction for $\alpha = \beta = 0$ *and* $\gamma < 0$*, that is, the linearization at the origin has the eigenvalues* 0 *and* $\pm i\sqrt{-\gamma}$.

We observe that the rescaling of time and u by

$$t \to c^2 t, \quad u_1 \to c^{-3} u_1, \quad u_2 \to c^{-5} u_2, \text{ and } \quad u_3 \to c^{-7} u_3$$

preserves the structure of the reduced model (22) completely but rescales the parameters as

$$\alpha \to c^6 \alpha, \quad \beta \to c^2 \beta, \text{ and } \quad \gamma \to c^4 \gamma.$$

Hence, system (22) has cone structure, and we can restrict the bifurcation analysis to the parameter sphere $\alpha^2 + \beta^2 + \gamma^2 = 1$. Let us introduce polar coordinates on this sphere:

$$\alpha = \sin \frac{\pi}{2}\varphi, \qquad \beta = \cos \frac{\pi}{2}\varphi \ \cos 2\pi\psi, \qquad \gamma = \cos \frac{\pi}{2}\varphi \ \sin 2\pi\psi. \tag{24}$$

This transformation maps the sphere onto the rectangle $[-1, 1] \times [0, 1] \ni (\varphi, \psi)$. It is singular at $\varphi = \pm 1$ and periodic in ψ with period one. Figure 4 shows the part of the upper half of the sphere where all bifurcation curves and surfaces intersect the sphere. In this world map like projection, the 'equator' is vertical and the 'poles' of the coordinates are at the left and right ends of the plot.

The pitchfork bifurcation plane intersects the sphere along its equator $\{\varphi = 0\}$. The line of double-zero singularities traverses the sphere along its diameter intersecting it in the points DZ_- at $(\varphi, \psi) = (0, 0.5)$ and DZ_+ at $(\varphi, \psi) = (0, 1)$. The line of pitchfork-Hopf interactions enters the sphere in PH_1 at $(\varphi, \psi) = (0, 0.75)$ and ends at its midpoint. The Hopf surface intersects the sphere in a curve ending in the double-zero singularities, and intersecting the pitchfork line (equator) in PH_1. The origin is linearly stable in region I in figure 4. This region is bounded by the pitchfork line $\varphi = 0$ and by a supercritical Hopf curve.

5.1. Bifurcations of symmetric periodic orbits

We explore the bifurcations of periodic orbits of (22) numerically using the standard bifurcation analysis tool AUTO [10]. Here it is particularly handy to work on the parameter sphere given by (24); see also [23]. The double-zero singularity DZ_- is transversally stable, that is, the third eigenvalue is negative according to Lemma 3. A heteroclinic bifurcation is born in DZ_- (dashed-double-dotted curve in figure 4). That is, a parameter curve emanates from DZ_- where an eye-shaped heteroclinic cycle connects the two saddles emerged from the pitchfork bifurcation; see case "$s = 1$" of the normal form analysis of the 1:2 resonance in Ref. [24]. The saddle characteristics change along the curve of heteroclinics in the (φ, ψ)-plane. There is a negative degenerate eigenvalue at DE, the saddles become neutral at NS (positive real eigenvalue, complex conjugate pair with negative real parts), and neutrally divergent at ND (at $\psi = 0.75$, see figure 4). Accordingly, the approach of the symmetric periodic orbits toward the heteroclinic cycle changes. In figure 5, we depict the one-parameter families of periodic

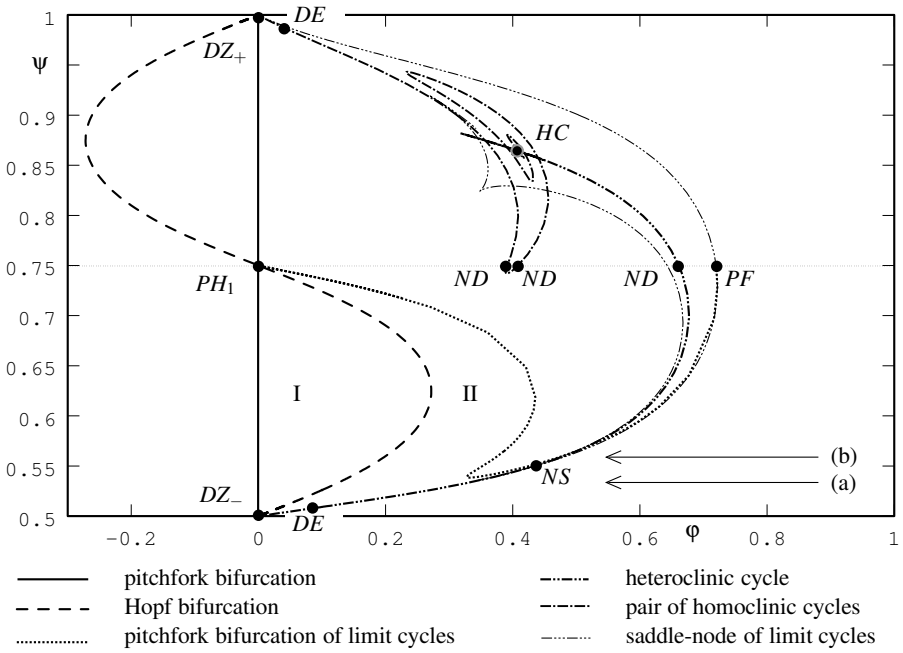

Figure 4. Bifurcations of the origin and of symmetric periodic orbits in the (φ, ψ)-plane of the reduced model (22).

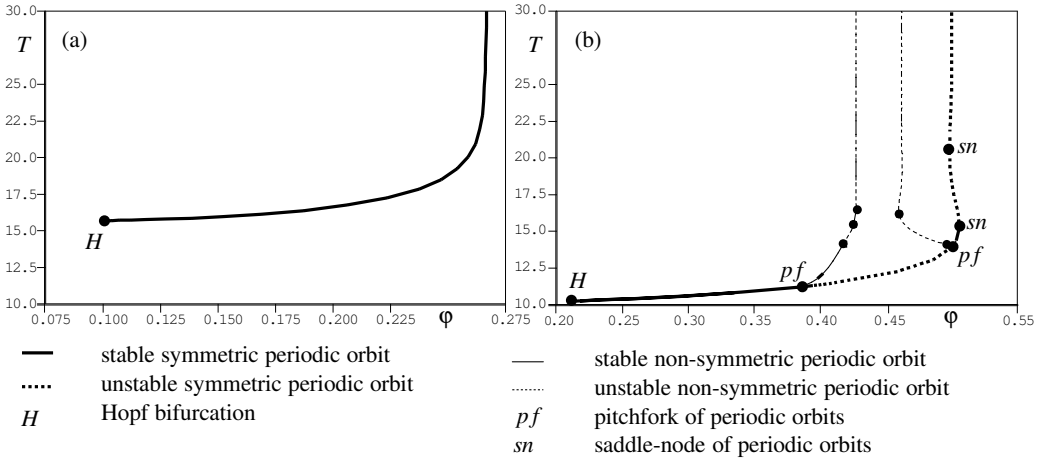

Figure 5. The period T of the symmetric periodic orbits as a function of φ for $\psi = 0.53$ where the saddle quantity at heteroclinic connection is negative (a), and for $\psi = 0.56$ where the saddle quantity is positive but the divergence at the heteroclinic connection is negative (b).

orbits for $\psi = \text{const}$ below and above the point NS; see figure 4 for the location of these cross-sections in the (φ, ψ)-plane. Figure 5(b) illustrates that there are infinitely many symmetric periodic orbits of stable and of saddle type in the vicinity of the curve of heteroclinics between NS and ND. That is, the family of symmetric periodic orbits undergoes an infinite sequence of pitchfork bifurcations and saddle-node bifurcations accumulating to the heteroclinic bifurcation. The first elements of this infinite sequence

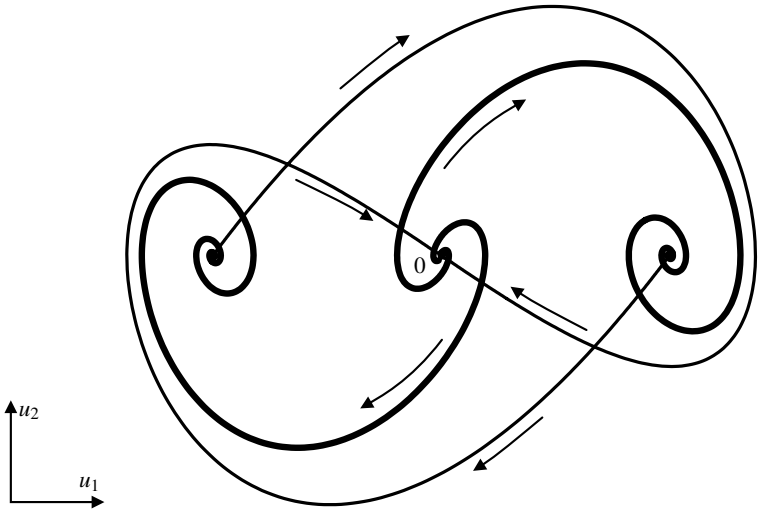

Figure 6. Phase portrait of the multiple heteroclinic chain at the parameter point HC in projection onto the (u_1, u_2)-plane, as computed with AUTO. The generic saddle-connections are drawn as bold curves.

are depicted as points in figure 5(b), where saddle-node bifurcations are labeled by sn and pitchfork bifurcations by pf. The non-symmetric periodic orbits emerging from the pitchfork bifurcations undergo further bifurcations and will be studied in section 5.2.

We have added the first pitchfork bifurcation of periodic orbits as a dotted curve and the first saddle-node bifurcation of periodic orbits as a thin dashed-triple-dotted curve in figure 4. These curves meet each other in a pitchfork-saddle-node interaction PF. This bifurcation has the same normal form as the Hopf-saddle-node bifurcation that is described in, for example, Ref. [24]. The Hopf curve, the first curve of pitchfork bifurcations of periodic orbits, the first curve of saddle-nodes of periodic orbits and the curve of heteroclinics form the boundaries of region II in figure 4, the biggest part of the island of stable symmetric periodic orbits.

The double-zero singularity DZ_+ is transversally unstable, that is, the third eigenvalue is positive. According to Ref. [24] (normal form for 1:2 resonance, case "$s = -1$"), a parameter curve is born in DZ_+ where a figure-eight pair of homoclinic connections to the origin exists. Along this curve of homoclinic orbits the saddle quantity of the origin changes several times. There is a positive degenerate eigenvalue in DE, and the origin is neutrally divergent in ND. We have depicted the curve of homoclinic orbits by a dashed-dotted curve in figure 4.

This curve of homoclinic orbits meets with the heteroclinic cycle born in DZ_- in the point HC. In this point, there exists a multiple heteroclinic chain $0 \to (\sqrt{\alpha}, 0, 0) \to 0 \to (-\sqrt{\alpha}, 0, 0) \to 0$. The phase portrait of this heteroclinic chain is depicted in figure 6. The heteroclinic chain consists of two generic saddle connections (bold curves) and of two codimension-two saddle connections. In parameter space, the curve of homoclinic orbits is spiraling toward the point HC. This type of codimension-two heteroclinic chain was first studied by Bykov in the context of generic vector fields without any

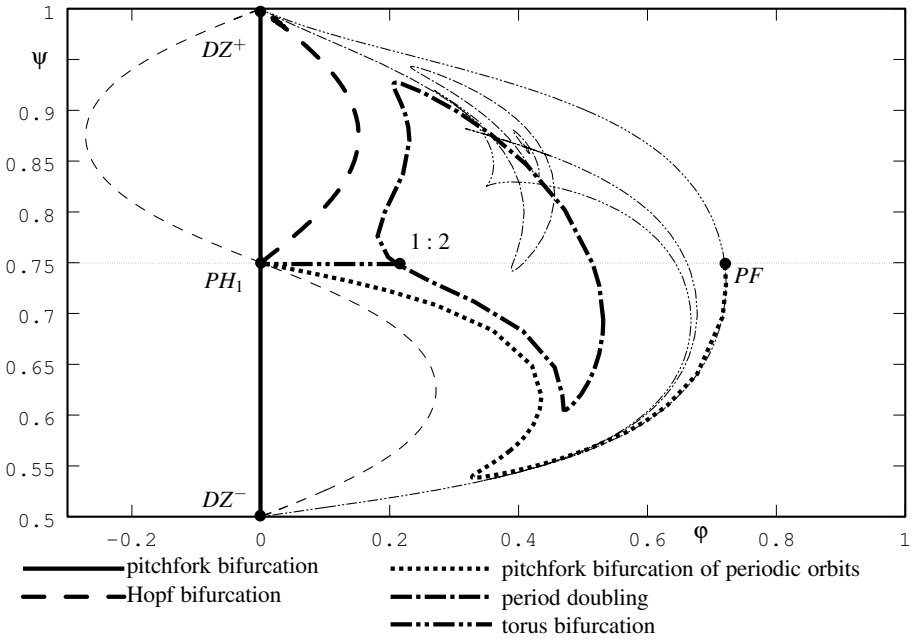

Figure 7. Bifurcations of non-symmetric equilibria and of non-symmetric periodic orbits in the (φ, ψ)-plane of the reduced model (22); the bifurcations of the origin and of symmetric periodic orbits from figure 4 are repeated for orientation.

extra symmetry [3, 4]. It was then found in systems with the $\mathbb{Z}_2$-symmetry of rotation by π around a fixed coordinate axis (for example, in the Lorenz system [16], and a DDE system describing a laser with phase-conjugate feedback [17]) where it is generally referred to as a T-point bifurcation [16]. This homoclinic chain or T-point bifurcation was also found in the point-reflection symmetric Chua equations in Refs. [1].

Finally, there is a curve of saddle-node bifurcations of periodic orbits born in DZ_+ shown as thin dashed-triple-dotted curve in figure 4.

In summary, we have found one contiguous two-parameter family of symmetric periodic orbits bordered by the Hopf curve and the curves of heteroclinic and homoclinic cycles in figure 4. The main part of the stability region is marked by II in figure 4 but there are also small tongues of stable symmetric periodic orbits close to the connecting cycles.

5.2. Bifurcations of non-symmetric equilibria and periodic orbits

Although the non-symmetric equilibria and periodic orbits do not correspond to successful balancing of the pendulum (see section 2), we investigate their basic bifurcations briefly since they are important for understanding the dynamics in the vicinity of a general triple-zero eigenvalue singularity with $\mathbb{Z}_2$-symmetry. Their bifurcations are shown in figure 7.

Any non-symmetric equilibrium, periodic orbit or homoclinic connection has a counterpart obtained by reflection at the origin. Consequently, each curve in

figure 7 refers to two symmetrically related objects in the phase space that bifurcate simultaneously.

We start to explore the non-symmetric bifurcations at the pitchfork-Hopf interaction PH_1 at $(\varphi, \psi) = (0, 0.75)$. The unfolding of PH_1 corresponds to the unfolding of the normal form flow of the non-resonant Hopf-Hopf interaction (see the section about Hopf-Hopf interactions in Ref. [24, case VI of the 'difficult' case]). A Hopf bifurcation of the non-symmetric saddles, a pitchfork bifurcation of symmetric periodic orbits, and a torus bifurcation curve emanate from PH_1. The curve of Hopf bifurcations of the non-symmetric saddles ends in DZ_+. The torus bifurcation ends in a $1:2$ resonance meeting a closed loop of period doubling bifurcations.

According to theory [24], there are infinitely many non-symmetric homoclinic connections to the non-symmetric saddles in the vicinity of the heteroclinic curve above the parameter point NS; see figure 4. The theory of dynamics in the vicinity of homoclinic orbits to saddle-foci applies to each of these homoclinic orbits. Hence, there are infinitely many non-symmetric periodic orbits undergoing sequences of period-doublings and saddle-node bifurcations in the vicinity of each of these homoclinic bifurcations. It is impossible to track the complicated dynamics and the infinitely many periodic orbits and bifurcations attached to these homoclinic orbits to saddle-foci.

The torus bifurcation curve coincides exactly with the meridian $\beta = 0$. Moreover, there exist families of invariant tori in the phase space along the torus bifurcation curve implying that the torus bifurcation is infinitely degenerate. Furthermore, we observe that along this meridian all equilibria are neutrally divergent saddles. This is numerical evidence that the truncated model (22) is conservative at $\beta = 0$. Hence, we would have to take into account terms of higher order in r in (21) in order to unfold the torus bifurcation of non-symmetric periodic orbits in the same way as in the Hopf-Hopf interaction in Ref. [24]. This is beyond the scope of this paper as it requires the computation of at least two expansion coefficients of the center manifold (see section 4.3) as done in Ref. [6].

6. Extension beyond the neighborhood of the singularity

Theorem 2 connects the results of the bifurcation analysis in section 5 to the dynamical system (14) for a sufficiently small neighborhood of the triple-zero eigenvalue singularity. In this section we investigate how the bifurcation diagram in figure 4 is affected by an increase of the scaling parameter r. Instead of expanding the higher-order term h_2 in (21), we explore the full DDE system (11)-(12) directly.

DDE-BIFTOOL [13] is a library of MATLAB routines capable of continuing equilibria, periodic orbits, and homoclinic/heteroclinic connections in DDEs, and monitoring eigenvalues or Floquet multipliers, respectively. This library allows us to perform a bifurcation analysis for the DDE system (11)-(12). However, this requires some additional scripting effort guided by the diagram in figure 4, since DDE-BIFTOOL in its current state can neither detect nor continue local bifurcations of periodic orbits

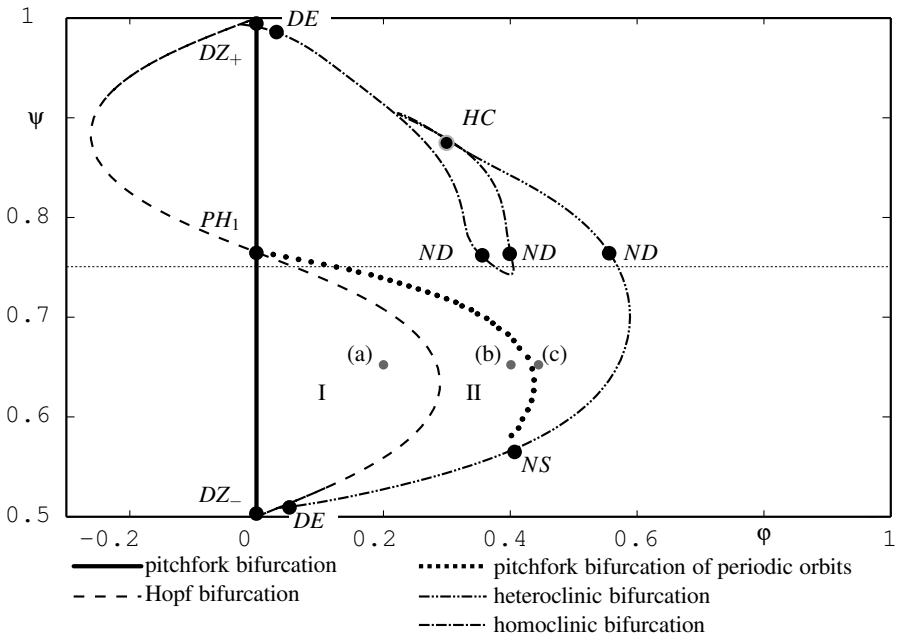

Figure 8. Bifurcation of equilibria and of symmetric periodic orbits in the (φ, ψ)-plane of the full DDE (5)–(6); compare figure 4.

automatically.

We choose $r = 0.5$ and $\varepsilon = 0$. The transformations (17) and (24) relate the (φ, ψ)-plane to an ellipsoid around λ_0 in the space of the original parameters.

The bifurcation diagram in figure 8 shows all bifurcations of the origin and of symmetric periodic orbits which can be continued using DDE-BIFTOOL, that is, all bifurcations of the origin and the heteroclinic and homoclinic bifurcations emerging from DZ_- and DZ_+. The region of linear stability of the origin and the primary region of stable symmetric periodic orbits are again marked by I and II, respectively. The connecting cycles are approximated by periodic orbits of large period (we used $T = 1.16e2$). This approximation is inaccurate close to the pitchfork-Hopf interactions DZ_- and DZ_+ and close to the point HC of the multiple heteroclinic chain. Hence, we have computed HC using the recently implemented DDE-BIFTOOL routines for saddle connections [29]; see also [17].

Moreover, we approximated the curve of pitchfork bifurcations of periodic orbits by checking the Floquet multipliers successively along families of symmetric periodic orbits for constant ψ. The dotted line in figure 8 shows the first step of the continuation where at least one Floquet multiplier is greater than 1.05. The parameter points marked (a)-(c) in figure 8 correspond to the time profiles shown in figure 2. In particular, the motion $\delta(t)$ of the cart accelerates when the curve of pitchfork bifurcations of periodic orbits is crossed, which physically means the loss of effective control of the system.

Since the computation of Floquet multipliers is very inaccurate for periodic orbits with long period we cannot detect the curves of saddle-nodes and pitchfork bifurcations close to the heteroclinic and homoclinic bifurcations in figure 8. However, according to

theory [24] there are infinitely many pitchfork and saddle-node bifurcations close to the parts of the homoclinic and heteroclinic orbits above NS in figure 8.

In summary, the bifurcation diagrams in figure 4 for the reduced system (22) and in figure 8 for the full DDE system (11)-(12) agree quantitatively even though the value $r = 0.5$ we chose in figure 8 is not very small. This shows that the triple-zero eigenvalue singularity is indeed an organizing center for the stable small amplitude dynamics of the full DDE system (11)-(12).

7. Conclusions and outlook

We have shown that the dynamics of an inverted pendulum on a cart subject to delayed linear control is organized by a triple-zero singularity. The partial unfolding by way of a three-dimensional ODE on the center manifold that we presented in the case of an extra $\mathbb{Z}_2$-symmetry is a contribution to the recent literature on this singularity. It was found to be valid even quite far away from the actual singularity in the full DDE. Our results show that small amplitude oscillations exist around the upright position of the pendulum. These solutions are $\mathbb{Z}_2$-symmetric and can be interpreted as successful, albeit not perfect, control of the pendulum. Bifurcating non-symmetric solutions correspond to a situation where the motion of the cart is unbounded, which is interpreted as a loss of effective control.

There remain several open questions. First of all, there are control-theoretic questions. Is it possible to construct controllers that stabilize small-amplitude motion for values of the delay τ above the critical delay τ_* where the singularity occurs? Can information obtained from the bifurcation diagrams presented here be useful to achieve this?

Secondly, there are questions concerning the unfolding of the triple-zero singularity for $\mathbb{Z}_2$-symmetric vector fields. We found evidence that there are families of invariant tori for $\beta = 0$ in the ODE model (22), so that the full unfolding will include other terms than we considered. Is the associated parameter locus where the ODE model is conservative related to the Kuramoto-Sivashinsky system that appears as a reversible limit in the suggested unfolding [14] of the triple-zero singularity in the generic case? What happens if more higher-order terms are added to unfold the singularity? More generally, what is the proper form of an unfolding, and up to which order does one have to go? Do the parameters of the original DDE model unfold the singularity or are there similar restrictions on the flow on the center manifold as were found in Ref. [2]?

Finally, the engineering point of view demands to advance to more realistic models, for example, to include the effects of a nonlinear spring into the system as studied in Ref. [21] (without extensive treatment of the delay). In particular, non-smooth (backlash) spring models are realistic but require a completely different approach to the investigation of the singularity.

In short, there remain many interesting questions for future research concerning this problem at the meeting point of mechanical engineering, control theory, the dynamics

of delay differential equations, and bifurcation theory.

Acknowledgments

The authors thank Gábor Stépán for helpful discussions and encouragement. The research of J.S. is supported by EPSRC grant GR/R72020/01.

References

[1] A. Algaba, M. Merino, E. Freire, E. Gamero, and A. Rodriguez-Luis. Some results on Chua's equation near a triple-zero linear degeneracy. *International Journal of Bifurcation and Chaos*, 13(3):583–608, 2003.

[2] P.-L. Buono and J. Bélair. Restrictions and unfolding of double Hopf bifurcation in functional differential equations. *Journal of Differential Equations*, 189:234–266, 2003.

[3] V.V. Bykov. Orbit structure in a neighborhood of a separatrix cycle containing two saddle foci. in *Methods of qualitative theory of differential equations and related topics*, *American Math. Soc. Transl. Ser 2*, 200:87-97, 2000.

[4] V.V. Bykov. The bifurcations of separatrix contours and chaos. *Physica D* 62:290–299, 1993.

[5] J. L. Cabrera and J. G. Milton. On-off intermittency in a human balancing task. *Physical Review Letters*, 89(158702), 2002.

[6] S. A. Campbell and J. Bélair. Analytical and symbolically-assisted investigation of Hopf bifurcation in delay-differential equations. *Canadian Applied Mathematics Quarterly*, 3(2):137–154, 1995.

[7] S. A. Campbell, J. Bélair, T. Ohira, and J. Milton. Complex dynamics and multistability in a damped harmonic oscillator with delayed negative feedback. *Chaos*, 5(4):640–645, 1995.

[8] B. Char, K. Geddes, G. Gonnet, B. Leong, M. Monagan, and S. Watt. *Maple V Language Reference Manual*. Springer-Verlag, New York, Heidelberg, Berlin, 1991.

[9] O. Diekmann, S. van Gils, S. M. Verduyn Lunel, and H.-O. Walther. *Delay Equations*, volume 110 of *Applied Mathematical Sciences*. Springer-Verlag, 1995.

[10] E. J. Doedel, A. R. Champneys, T. F. Fairgrieve, Y. A. Kuznetsov, B. Sandstede, and X. Wang. *AUTO97, Continuation and bifurcation software for ordinary differential equations*, 1998.

[11] F. Dumortier and S. Ibañez. Nilpotent Singularities in Generic 4-Parameter Families of 3-Dimensional Vector Fields. *Journal of Differential Equations*, 127:590–647, 1996.

[12] F. Dumortier, S. Ibañez, and H. Kokubu. New aspects in the unfolding of the nilpotent singularity of codimension three. *Dynamical Systems*, 16(1):63–95, 2001.

[13] K. Engelborghs, T. Luzyanina, and G. Samaey. DDE-BIFTOOL v.2.00: a Matlab package for bifurcation analysis of delay differential equations. Report TW 330, Katholieke Universiteit Leuven, 2001.

[14] E. Freire, E. Gamero, A. J. Rodriguez-Luis, and A. Algaba. A note on the triple-zero linear degeneracy: Normal forms, dynamical and bifurcation behaviors of an unfolding. *Int. J. of Bifurcation and Chaos*, 12(12):2799–2820, 2002.

[15] M. Garcia, A. Chatterjee, and A. Ruina. Efficiency, speed, and scaling of passive dynamical bipedal walking. *Dynamics and Stability of Systems*, 15(2):75–99, 2000.

[16] P. Glendinning and C. Sparrow. T-Points: A codimension two heteroclinic bifurcation. *Journal of Statistical Physics*, 43:479–488, 1986.

[17] K. Green, B. Krauskopf, and G. Samaey. A two-parameter study of the locking region of a semiconductor laser subject to phase-conjugate feedback. *SIAM J. of Appl. Dyn. Sys.*, 2:254–276, 2003.

[18] J. K. Hale and S. M. Verduyn Lunel. *Introduction to Functional Differential Equations*, volume 99 of *Applied Mathematical Sciences*. Springer-Verlag, 1993.

[19] M. Hirsch, C. Pugh, and M.Shub. *Invariant Manifolds.* Springer Verlag, Berlin, 1977.

[20] T. Kato. *Perturbation Theory for Linear Operators.* Springer Verlag, 1966.

[21] L. E. Kollár, G. Stépán, and S. J. Hogan. Sampling delay and backlash in balancing systems. *Periodica Polytechnica Ser. Mech. Eng.*, 44(1):77–84, 2000.

[22] B. Krauskopf and D. Lenstra, editors. *Fundamental Issues of Nonlinear Laser Dynamics.* American Institute of Physics, 2000.

[23] B. Krauskopf and C. Rousseau. Codimension-three unfoldings of reflectionally symmetric planar vector fields. *Nonlinearity*, 10(5):1115–1150, 1997.

[24] Y. Kuznetsov. *Elements of Applied Bifurcation Theory.* Springer Verlag, 1995.

[25] C. M. Marcus and R. M. Westervelt. Stability of analog networks with delay. *Phys. Rev. A*, 39:347–359, 1989.

[26] N. Minorsky. *Nonlinear Oscillations.* D. Van Nostrand, Princeton, 1962.

[27] F. C. Moon. *Dynamics and Chaos in Manufacturing Processes.* Wiley, New York, 1998.

[28] A. Pazy. *Semigroups of Linear Operators and Applications to Partial Differential Equations.* Applied mathematical Sciences. Springer Verlag, New York, 1983.

[29] G. Samaey, K. Engelborghs, and D. Roose. Numerical computation of connecting orbits in delay differential equations. *Numer. Algorithms*, 30:335–352, 2002.

[30] L. P. Shayer and S. A. Campbell. Stability, bifurcation, and multistability in a system of two coupled neurons with multiple time delays. *SIAM J. of Appl. Math.*, 61(2):673–700, 2000.

[31] G. Stepán. *Retarded Dynamical Systems: Stability and Characteristic Functions.* Longman Scientific and Technical, 1989.